Ceilometer Observation of a Dust Event in the Gobi Desert on 29–30 April 2015: Sudden Arrival of a Developed Dust Storm and Trapping of Dust Within an Inversion Layer

Kei Kawai[1], Yuta Nishio[2], Kenji Kai[1, 3], Jun Noda[4], Erdenebadrakh Munkhjargal[1, 5], Masato Shinoda[1], Nobuo Sugimoto[6], Atsushi Shimizu[6], Enkhbaatar Davaanyam[5, 7], and Dashdondog Batdorj[8]

[1]*Graduate School of Environmental Studies, Nagoya University, Nagoya, Japan*
[2]*Japan Meteorological Agency, Tokyo, Japan*
[3]*Ibaraki University, Mito, Japan*
[4]*Rakuno Gakuen University, Ebetsu, Japan*
[5]*Information and Research Institute of Meteorology, Hydrology and Environment, Ulaanbaatar, Mongolia*
[6]*National Institute for Environmental Studies, Tsukuba, Japan*
[7]*University of Tsukuba, Tsukuba, Japan*
[8]*National Agency for Meteorology and Environmental Monitoring, Ulaanbaatar, Mongolia*

Abstract

Asian dust is transported over a long range via the mid-latitude westerlies when dust is lifted to the free troposphere over the source regions, whereas dust remaining in the atmospheric boundary layer is not transported far. In the Gobi Desert, a major source region of Asian dust, a ceilometer (compact lidar) monitors the vertical distribution of dust at Dalanzadgad, Mongolia. On 29−30 April 2015, the ceilometer observed a developed dust storm over the ground, followed by a dust layer within a height of 1.2−1.8 km. The dust storm had already developed in the upwind region before reaching Dalanzadgad. This feature was also shown in the ceilometer observation data. The dust layer remained at almost the same height for 12 h, because the dust became trapped within an inversion layer at a height of 1.2−1.5 km over cold air. This result suggests that the inversion layer prevented the dust from reaching the free troposphere, thereby restraining the long-range transport of the dust via the westerlies. This is the first paper that reports this type of vertical distribution of dust in the source region based on observation data.

(**Citation**: Kawai, K., Y. Nishio, K. Kai, J. Noda, E. Munkhjargal, M. Shinoda, N. Sugimoto, A. Shimizu, E. Davaanyam, and D. Batdorj, 2019: Ceilometer observation of a dust event in the Gobi Desert on 29−30 April 2015: Sudden arrival of a developed dust storm and trapping of dust within an inversion layer. *SOLA*, **15**, 52−56, doi:10.2151/sola.2019-011.)

1. Introduction

Asian dust, a type of mineral aerosol, has impacts on climate (Huang et al. 2014) and human health (Higashi et al. 2014). Asian dust is blown from the ground surface into the atmospheric boundary layer (ABL) in arid and semi-arid regions of East Asia, such as the Gobi Desert, Taklimakan Desert, and Loess Plateau (Sun et al. 2001; Kurosaki and Mikami 2005; Wu et al. 2016). If dust is lifted to the free troposphere (FT), it is transported over a long range toward the North Pacific via the mid-latitude westerlies (Kai et al. 1988; Husar et al. 2001; Uno et al. 2009; Yumimoto et al. 2009). Conversely, dust that remains within the ABL is not transported far (Hara et al. 2009). Thus, the long-range transport of dust is strongly related to its vertical distribution in the source region.

The vertical distribution of dust is most effectively observed using lidar (light detection and ranging), which is an active remote-sensing instrument that uses pulsed laser beams with high spatiotemporal resolutions. As an international collaborative research between Japan and Mongolia, we installed a ceilometer (i.e., compact lidar) in the Gobi Desert (Dalanzadgad, Mongolia) at the end of April 2013. The resulting ceilometer observation data were used to analyze dust events in May 2013 (Kawai et al. 2015; Kawai et al. 2018) and May 2017 (Minamoto et al. 2018).

In the Gobi Desert, most dust events are caused by low pressures or cold fronts (Shao and Wang 2003; Takemi and Seino 2005). For instance, in our previous studies (Kawai et al. 2015; Kawai et al. 2018), we showed that a cold frontal system transported dust from the ground surface through the ABL to the FT over the Gobi Desert. However, information on the vertical distribution of dust in the source region is still lacking. Therefore, additional dust events should be analyzed using observation data, and the findings should be synthesized with existing knowledge.

On 29−30 April 2015, the ceilometer observed a dust storm over the ground, followed by a dust layer floating within a height of 1.2−1.8 km for 12 h. The dust did not appear to reach the FT. In this paper, we describe the characteristics of the dust storm and the floating dust layer to determine the atmospheric condition that prevented the dust from reaching the FT. This paper presents the first description of this type of vertical distribution of dust in the source region based on observation data.

2. Observations and data

A ceilometer observation has been conducted at Dalanzadgad, Mongolia, located in the central part of the Gobi Desert (43.58°N, 104.42°E, 1470 m a.s.l.; Fig. 1). The ceilometer (CL51; Vaisala, Vantaa, Finland) uses a diode laser at a wavelength of 910 nm. A profile of attenuated backscatter coefficients below a height of 15.4 km with a height resolution of 10 m is outputted to a laptop computer every 6 s. In this study, we used the 1-min-averaged profiles. The observational capability of the ceilometer for dust was confirmed by Jin et al. (2015).

PM_{10} and $PM_{2.5}$ mass concentrations are measured at a height of 4 m at Dalanzadgad (Jugder et al. 2014). We used these concentrations averaged over 1 h. We measured the size-resolved number concentrations of aerosol particles with an optical particle counter (OPC; AeroTrak 9306-V2; TSI, Shoreview, MN, USA) with six channels (0.3, 0.5, 1, 3, 5, and 10 μm) at Dalanzadgad.

To determine the weather conditions, we used SYNOP data, including temperature, dew point temperature, wind speed and direction, and present weather (WMO 2011). The present weather codes were used to identify dust phenomena (06: floating dust; 07, 08: blowing dust; 09, 30−35, 98: dust storm). We also analyzed

Corresponding author: Kei Kawai, Nagoya University, Furo-cho, Chikusa-ku, Nagoya 464-8601, Japan. E-mail: kawai.kei@e.mbox.nagoya-u.ac.jp.

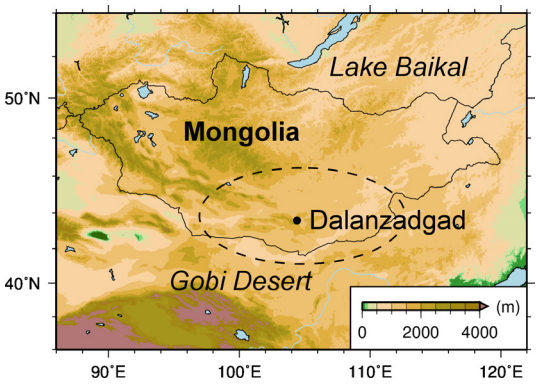

Fig. 1. Topographic map of Mongolia. The color scale in the lower right legend represents altitude.

routine radiosonde observation data at Dalanzadgad. The observed relative humidity was used to distinguish dust from cloud. In addition, we analyzed the National Centers for Environmental Prediction (NCEP, USA) Final (FNL) Operational Global Analysis data in 1° × 1° grids. The local standard time (LST) used in this study was 8 h ahead of the Coordinated Universal Time (UTC).

3. Results

3.1 Field observations

A dust storm was observed at Dalanzadgad from 19 LST on 29 April 2015. During the dust storm, the landscape took on a yellow to brown hue, the horizontal visibility decreased to about 150 m, and distant mountains were not visible (Fig. 2a; Supplement 1). After the dust storm, on the morning of 30 April, the horizontal visibility recovered to more than 20 km, and the distant mountains became visible (Fig. 2b). By contrast, the sky was still hazy due to the presence of a floating dust layer mentioned below.

We conducted OPC observations at Dalanzadgad during and after the dust storm to indicate its characteristic in quantitative manner (Fig. 3). The particle number concentrations in the whole measured size range were higher during than after the dust storm. In particular, the ratios of particles with a diameter greater than 0.7 μm were 88−137. Mikami et al. (2005) also showed that the number of coarse particles (3−5 μm) increased more than that of fine particles (0.3−0.5 μm) during dust storms in the Taklimakan Desert. These OPC observation data are helpful to research on dust emission, for instance, using numerical simulation.

3.2 Ceilometer and other observations

Figure 4a shows the time-height cross section of the ceilometer observation data at Dalanzadgad. The dust storm was represented by large attenuated backscatter coefficients (> 1.5 × 10^{-3} km^{-1} sr^{-1}) over the ground between 19 LST on 29 April and 02 LST on 30 April (mark A in Fig. 4a). The top height of the dust storm reached 1.3 km at 23 LST on 29 April. The upper part of the dust storm between 19 LST and 22 LST on 29 April may not have been observed due to the full attenuation of the laser pulses emitted by the ceilometer and the backscattered light.

Figure 4b presents the temporal variations in PM_{10} and $PM_{2.5}$ mass concentrations measured at Dalanzadgad. Because of the dust storm, the PM_{10} ($PM_{2.5}$) concentration drastically increased from 13 (8) μg m^{-3} at 18−19 LST to 743 (400) μg m^{-3} at 19−20 LST on 29 April, representing an increase of 57 (50) times over 1 h. These increases are consistent with Jugder et al. (2014), who mentioned that dust storms in the Gobi Desert caused increases in PM_{10} and $PM_{2.5}$ concentrations of two times to several tens of times. After that, the PM_{10} ($PM_{2.5}$) concentration gradually decreased to 20 (11) μg m^{-3} until 02 LST on 30 April. These variations corresponded to those of the attenuated backscatter coefficients near the ground observed by the ceilometer.

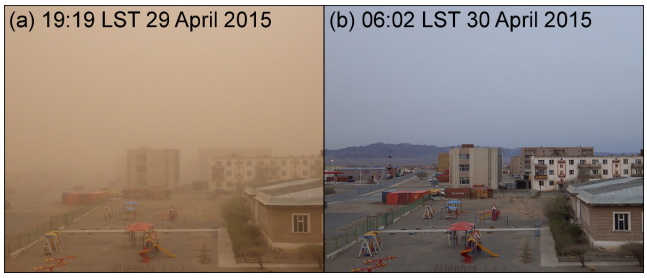

Fig. 2. Landscape photographs taken in Dalanzadgad toward the southwest (a) at 19:19 LST on 29 April and (b) at 06:02 LST on 30 April 2015.

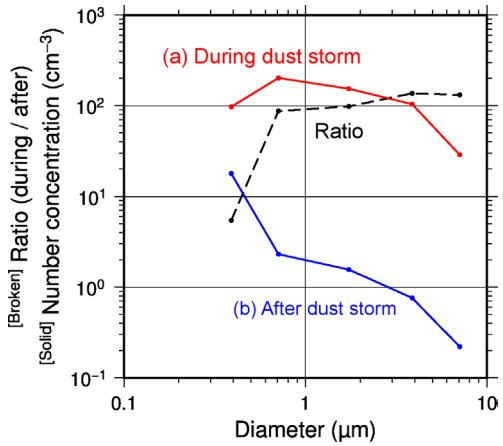

Fig. 3. Size-resolved number concentrations of aerosol particles observed by the optical particle counter at Dalanzadgad (a) during (21:09 LST on 29 April) and (b) after the dust storm (07:46 LST on 30 April 2015). The broken line indicates the ratio (during/after).

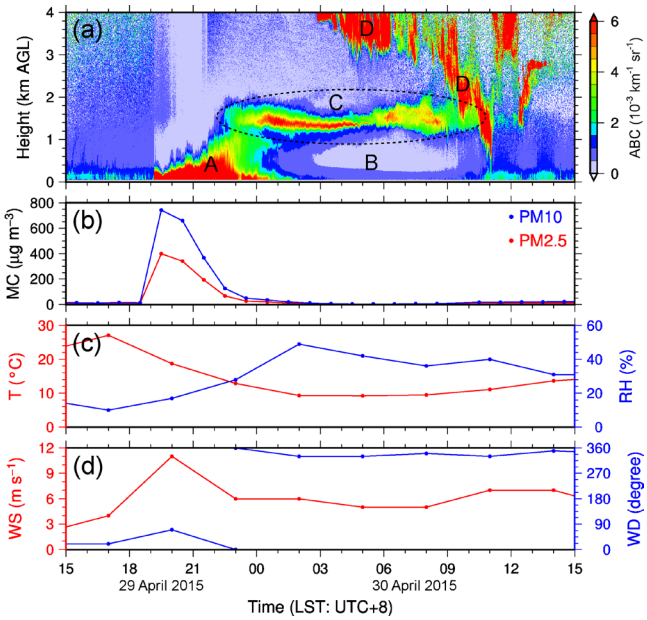

Fig. 4. Results of the ceilometer and surface observations at Dalanzadgad on 29−30 April 2015. (a) Time-height cross section of attenuated backscatter coefficients (ABC) from the ground to a height of 4 km above ground level (AGL) observed by the ceilometer. The letters A−D mark the dust storm, clean air, floating dust layer, and clouds, respectively. (b−d) Time-series of $PM_{2.5}$ and PM_{10} mass concentrations (MC), temperature (T), relative humidity (RH), wind speed (WS), and wind direction (WD).

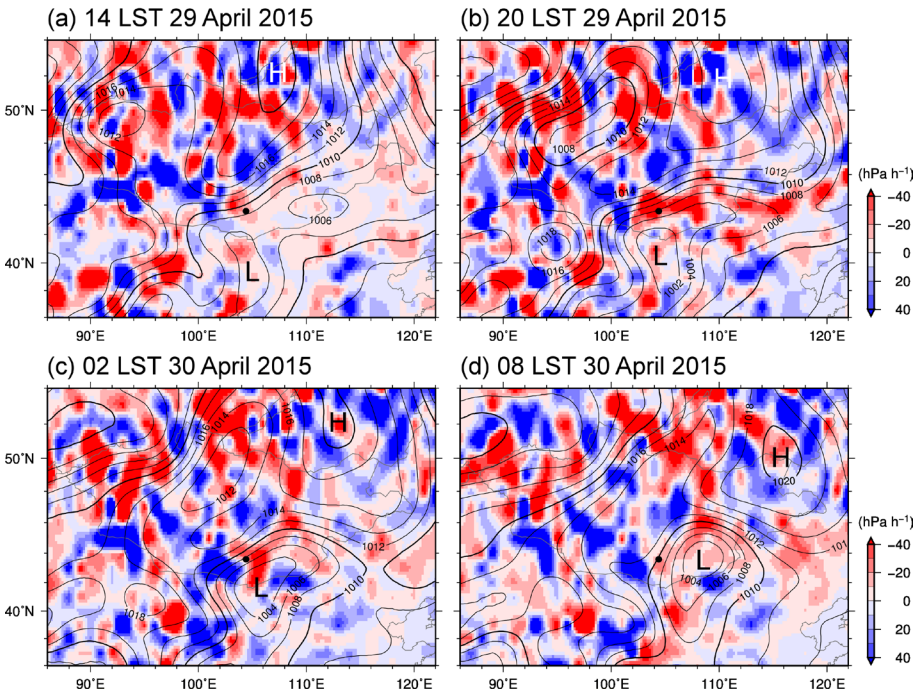

Fig. 5. Horizontal distributions of sea-level pressure (contours; every 2 hPa) and vertical velocity at 800 hPa (color gradient) around Mongolia on 29−30 April 2015 obtained from the NCEP FNL data. For vertical velocity, a negative value (red) indicates ascending motion, while a positive value (blue) indicates descending motion. The black dots show the location of Dalanzadgad.

Figures 4c and 4d present the meteorological observation data at Dalanzadgad. The temperature decreased from 27.1°C at 17 LST on 29 April to 9.3°C at 02 LST on 30 April (Fig. 4c). This large temperature decrease (−17.8°C) represented cold air advection. During the dust storm, the relative humidity was 17−49% (Fig. 4c), the wind speed was 6−11 m s^{-1}, and the wind direction rotated from east to north-northwest (Fig. 4d).

After the dust storm, the attenuated backscatter coefficients below a height of 1.2 km became small (0.0−1.0 × 10^{-3} km^{-1} sr^{-1}) (mark B in Fig. 4a), representative of clean air containing few dust particles. This clean air resulted in the recovery of horizontal visibility (Fig. 2b) and a low PM_{10} ($PM_{2.5}$) concentration of about 6 (4) μg m^{-3} (Fig. 4b).

A dust layer was indicated by relatively large attenuated backscatter coefficients (1.5−7.0 × 10^{-3} km^{-1} sr^{-1}) within a height of 1.2−1.8 km from 22:30 LST on 29 April to 10:30 LST on 30 April (mark C in Fig. 4a). The height of the floating dust layer remained almost unchanged for 12 h. The dust layer was connected to the top of the dust storm. The hazy sky after the dust storm (Fig. 2b) resulted from this floating dust layer.

The vertical structure of the dust layer had a different appearance before and after 05 LST on 30 April. During the former period, the thickness of the dust layer decreased from 0.6 to 0.3 km. The dust was densest near a height of 1.4 km according to the attenuated backscatter coefficients. During the latter period, the thickness of the dust layer increased again to about 0.6 km. The attenuated backscatter coefficients of the dust layer were relatively uniform, showing the presence of vertical mixing.

Clouds are shown by large attenuated backscatter coefficients (> 4.0 × 10^{-3} km^{-1} sr^{-1}) above a height of 0.6 km between 02 LST and 14 LST on 30 April (mark D in Fig. 4a). The height of clouds decreased from 4 km at 08 LST to 1 km at 11 LST. The thicknesses of the clouds were about 1 km. After 09:30 LST, the clouds appeared to mix with the floating dust. Kawai et al. (2018) also showed this kind of mixing during the dust event on 22−23 May 2013 and suggested that dust particles acted as ice nuclei based on the volume depolarization ratio observed by lidar.

3.3 Meteorological condition

Figure 5 shows the horizontal distributions of sea-level pressure and vertical velocity at 800 hPa over Mongolia obtained from the NCEP FNL data. At 14 LST on 29 April, a high pressure (central pressure: 1020 hPa) was located near Lake Baikal, while a low pressure (central pressure: 1006 hPa) was located to the south of Dalanzadgad (Fig. 5a). Thereafter, the high and low pressures moved southeastward and northeastward, respectively (Figs. 5b, 5c, and 5d). Due to the presence of these high and low pressures, the horizontal pressure gradient over Dalanzadgad was large, which resulted in the strong wind (Fig. 4d) and hence the dust storm (Fig. 4a).

During the dust storm, Dalanzadgad was located in the northern area of the low pressure (Fig. 5b). This atmospheric condition differed from that during the dust event on 22−23 May 2013, which was caused by a cold frontal system in the southwestern part of a low pressure (Kawai et al. 2015; Kawai et al. 2018).

During the dust storm, ascending air was distributed around Dalanzadgad at 800 hPa (Fig. 5b). This height corresponded to a height of about 0.5 km above ground level around Dalanzadgad. This ascending air should have lifted dust particles from the dust storm to the height of the floating dust layer.

4. Discussion

4.1 Sudden arrival of a developed dust storm

The attenuated backscatter coefficients near the ground observed by the ceilometer suddenly increased because of the dust storm (Fig. 4a). For example, the values at a height of 150 m increased by about 15 times over 1 min from 19:09 LST to 19:10 LST on 29 April. This feature differed from those of the dust storms on 22−23 May 2013 (Kawai et al. 2015; Kawai et al. 2018) and 2−4 May 2017 (Minamoto et al. 2018). In these cases, the attenuated backscatter coefficients near the ground gradually increased over a few hours, showing the gradual development of the dust storms at Dalanzadgad. Therefore, we consider that the dust storm analyzed in this study had already developed before reaching Dalanzadgad.

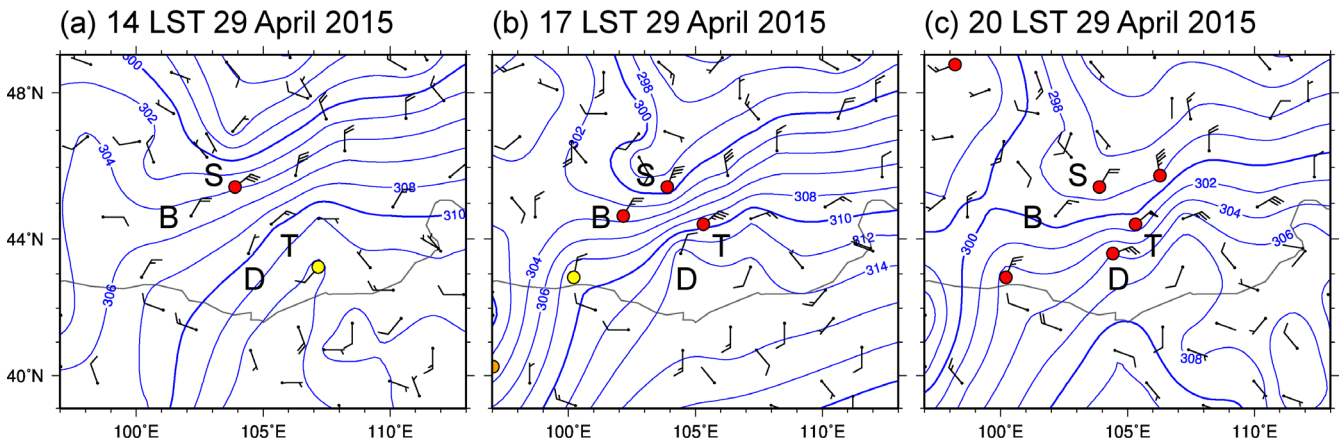

Fig. 6. Horizontal distributions of potential temperature (blue contours; every 2 K), surface wind, and dust phenomena observed over the Gobi Desert on 29 April 2015. The half and full barbs and the pennants represent wind speeds of 1, 2, and 10 m s^{-1}, respectively. The red-filled, orange-filled, and yellow-filled circles indicate dust storm, blowing dust, and floating dust, respectively. The letters S, B, T, and D represent Saikhan-Ovoo, Bogd, Tsogt-Ovoo, and Dalanzadgad, respectively.

This inference about the developed dust storm was confirmed by the horizontal distributions of surface wind and dust phenomena observed in the Gobi Desert on 29 April (Fig. 6). At 14 LST, a dust storm was observed at Saikhan-Ovoo with a northeast wind of 12 m s^{-1} (Fig. 6a). At 17 LST, the dust storm was also observed at Bogd and Tsogt-Ovoo with northeast winds of 11 and 14 m s^{-1}, respectively (Fig. 6b). The distribution area of the dust storm extended with the strong northeast wind. At 20 LST, the dust storm was finally observed at Dalanzadgad (Fig. 6c). Because Dalanzadgad is located 118 km southwest of Tsogt-Ovoo, the northeast wind observed at Tsogt-Ovoo at 17 LST reached Dalanzadgad after about 2 h. These results show that the dust storm observed at Dalanzadgad came from the upwind region with the strong northeast wind. This fact is consistent with the inference based on the ceilometer observation data. From the perspective of disasters, the sudden appearance of a dust storm is more dangerous than the gradual development, because of the minimal time for evacuation without forecast information.

The horizontal distributions of potential temperature observed on the ground over the Gobi Desert are shown in Fig. 6. It seems that the extension of the dust storm was accompanied by cold air advection. According to the ceilometer observation data (Fig. 4a), the developed dust storm likely had a clear leading edge like a gravity current (Simpson 1999). The leading edge of the dust storm may have corresponded to that of the advecting cold air, though observation data with high spatiotemporal resolution are lacking to confirm this.

4.2 Trapping of dust within an inversion layer

To investigate the atmospheric condition that maintained the floating dust layer at almost the same height for 12 h, we analyzed the radiosonde observation data at Dalanzadgad at 07:15 LST on 30 April (Fig. 7). The temperature profile showed an inversion layer at a height of 1.2−1.5 km over the cold air (Fig. 7a). In the inversion layer, the vertical gradient of the potential temperature was 6.5 K in a height range of 0.3 km (21.7 K km^{-1}), showing high atmospheric static stability.

The height of the inversion layer was almost the same as that of the floating dust layer, especially that of the vertical peak of the dust layer during the former period (1.4 km). It is suggested that the dust layer was captured into the inversion layer, resulting in the maintenance at almost the same height for 12 h. In other words, dust was unable to reenter the ABL or enter the FT because of the strong stability of the inversion layer. According to the potential temperature profile in Fig. 7a, if an air parcel in the inversion layer descends (ascends), it ascends (descends) back due to buoyancy. Although the dust protruded slightly above the inversion layer during the former period, this may have been due to inertia of the ascending dust.

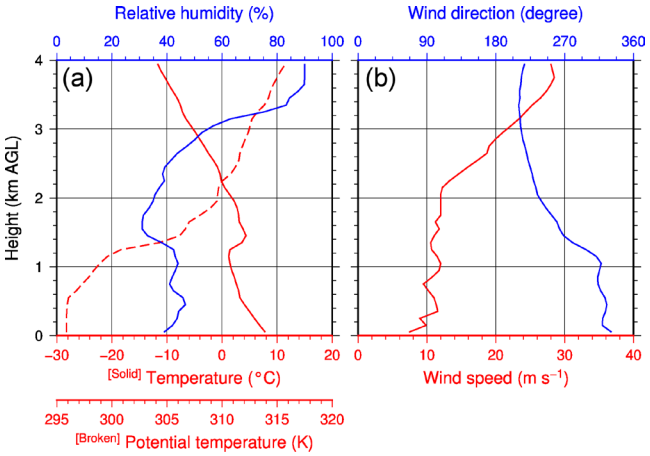

Fig. 7. Vertical profiles of (a) temperature, potential temperature, relative humidity, (b) wind speed, and wind direction from the ground to a height of 4 km obtained from radiosonde observation data at Dalanzadgad at 07:15 LST on 30 April 2015.

In the dust layer at 07:15 LST on 30 April, the relative humidity was 30−45% (Fig. 7a), the wind speed was 10−12 m s^{-1}, and the wind direction varied between northwest and southwest (Fig. 7b). Assuming that these wind conditions were constant for 12 h (equivalent to the duration of the observed dust layer), the dust layer would have a horizontal scale of about 430−520 km. However, the actual horizontal scale of the dust layer should be investigated using satellite observation data (e.g., Minamoto et al. 2018). In the FT over the dust layer, the southwest wind of 12−28 m s^{-1} corresponded to the mid-latitude westerlies. Thus, if not for the presence of the inversion layer, the dust would have reached the FT and have been transported over a long range via the westerlies. As future work, the mechanism by which the dust entered the stable inversion layer should be analyzed in detail using a regional numerical model (e.g., Takemi et al. 2006).

5. Conclusions

The ceilometer at Dalanzadgad, Mongolia, in the Gobi Desert observed a dust storm over the ground, followed by a dust layer floating at a height of 1.2−1.8 km on 29−30 April 2015. The dust

storm had already developed in the upwind region before reaching Dalanzadgad, which was also shown in the ceilometer observation data. The dust layer remained at almost the same height for 12 h, because the dust was captured within an inversion layer at a height of 1.2−1.5 km over cold air. It is suggested that the inversion layer prevented the dust from reaching the FT, restraining the long-range transport of the dust by the westerlies. This is the first report of this type of vertical distribution of dust in the source region based on observation data. As future work, satellite data analyses and numerical simulations are necessary for a more detailed understanding of this phenomenon.

Acknowledgements

The ceilometer observation at Dalanzadgad is supported by the Dalanzadgad Meteorological Observatory. The SYNOP data were provided by the National Centers for Environmental Information, National Oceanic and Atmospheric Administration, United States (https://www.ncdc.noaa.gov/isd). The NCEP FNL Operational Global Analysis data were obtained from the website (https://rda.ucar.edu/datasets/ds083.2/). This study was supported by Research Fellowships of Japan Society for the Promotion of Science (JSPS) for Young Scientists and by Grants-in-Aid for Scientific Research from the JSPS (16H02703, 17H01616, and 18J12795).

Edited by: T. Yasunari

Supplement

Supplement 1 is a video taken during the dust storm at Dalanzadgad, Mongolia, at 19:40 LST on 29 April 2015.

References

Hara, Y., K. Yumimoto, I. Uno, A. Shimizu, N. Sugimoto, Z. Liu, and D. M. Winker, 2009: Asian dust outflow in the PBL and free atmosphere retrieved by NASA CALIPSO and an assimilated dust transport model. *Atmos. Chem. Phys.*, **9**, 1227−1239.

Higashi, T., Y. Kambayashi, N. Ohkura, M. Fujimura, S. Nakanishi, T. Yoshizaki, K. Saijoh, K. Hayakawa, F. Kobayashi, Y. Michigami, Y. Hitomi, and H. Nakamura, 2014: Exacerbation of daily cough and allergic symptoms in adult patients with chronic cough by Asian dust: A hospital-based study in Kanazawa. *Atmos. Environ.*, **97**, 537−543.

Huang, J., T. Wang, W. Wang, Z. Li, and H. Yan, 2014: Climate effects of dust aerosols over East Asian arid and semiarid regions. *J. Geophys. Res.*, **119**, 11398−11416.

Husar, R. B., D. M. Tratt, B. A. Schichtel, S. R. Falke, F. Li, D. Jaffe, S. Gassó, T. Gill, N. S. Laulainen, F. Lu, M. C. Reheis, Y. Chun, D. Westphal, B. N. Holben, C. Gueymard, I. McKendry, N. Kuring, G. C. Feldman, C. McClain, R. J. Frouin, J. Merrill, D. DuBois, F. Vignola, T. Murayama, S. Nickovic, W. E. Wilson, K. Sassen, N. Sugimoto, and W. C. Malm, 2001: Asian dust events of April 1998. *J. Geophys. Res.*, **106**, 18317−18330.

Jin, Y., K. Kai, K. Kawai, T. Nagai, T. Sakai, A. Yamazaki, A. Uchiyama, D. Batdorj, N. Sugimoto, and T. Nishizawa, 2015: Ceilometer calibration for retrieval of aerosol optical properties. *J. Quant. Spectrosc. Radiat. Transfer*, **153**, 49−56.

Jugder, D., M. Shinoda, R. Kimura, A. Batbold, and D. Amarjargal, 2014: Quantitative analysis on windblown dust concentrations of PM_{10} ($PM_{2.5}$) during dust events in Mongolia. *Aeolian Res.*, **14**, 3−13.

Kai, K., Y. Okada, O. Uchino, I. Tabata, H. Nakamura, T. Takasugi, and Y. Nikaidou, 1988: Lidar observation and numerical simulation of a Kosa (Asian Dust) over Tsukuba, Japan during the Spring of 1986. *J. Meteor. Soc. Japan*, **66**, 457−472.

Kawai, K., K. Kai, Y. Jin, N. Sugimoto, and D. Batdorj, 2015: Dust event in the Gobi Desert on 22−23 May 2013: Transport of dust from the atmospheric boundary layer to the free troposphere by a cold front. *SOLA*, **11**, 156−159.

Kawai, K., K. Kai, Y. Jin, N. Sugimoto, and D. Batdorj, 2018: Lidar network observation of dust layer development over the Gobi Desert in association with a cold frontal system on 22−23 May 2013. *J. Meteor. Soc. Japan*, **96**, 255−268.

Kurosaki, Y., and M. Mikami, 2005: Regional difference in the characteristic of dust event in East Asia: Threshold wind speed for dust emission in east Asia and its seasonal variations. *J. Meteor. Soc. Japan*, **83A**, 1−18.

Mikami, M., T. Aoki, M. Ishizuka, S. Yabuki, Y. Yamada, W. Gao, and F. Zeng, 2005: Observation of number concentration of desert aerosols in the south of the Taklimakan Desert, China. *J. Meteor. Soc. Japan*, **83A**, 31−43.

Minamoto, Y., K. Nakamura, M. Wang, K. Kawai, K. Ohara, J. Noda, E. Davaanyam, N. Sugimoto, and K. Kai, 2018: Large-scale dust event in East Asia in May 2017: Dust emission and transport from multiple source regions. *SOLA*, **14**, 33−38.

Simpson, J. E., 1999: *Gravity Currents: In the Environment and the Laboratory, 2nd Edition*. Cambridge University Press, 244 pp.

Shao, Y., and J. Wang, 2003: A climatology of Northeast Asian dust events. *Meteorol. Z.*, **12**, 187−196.

Sun, J., M. Zhang, and T. Liu, 2001: Spatial and temporal characteristics of dust storms in China and its surrounding regions, 1960−1999: Relations to source area and climate. *J. Geophys. Res.*, **106**, 10325−10333.

Takemi, T., M. Yasui, J. Zhou, and L. Liu, 2006: Role of boundary layer and cumulus convection on dust emission and transport over a midlatitude desert area. *J. Geophys. Res.*, **111**, D11203.

Takemi, T., and N. Seino, 2005: Dust storms and cyclone tracks over the arid regions in east Asia in spring. *J. Geophys. Res.*, **110**, D18S11.

Uno, I., K. Eguchi, K. Yumimoto, T. Takemura, A. Shimizu, M. Uematsu, Z. Liu, Z. Wang, Y. Hara, and N. Sugimoto, 2009: Asian dust transported one full circuit around the globe. *Nat. Geosci.*, **2**, 557−560.

World Meteorological Organization (WMO), 2011: *Manual on codes, International codes, vol. I.1, Annex II to the WMO technical regulations, part A, Alphanumeric codes, 2011 edition*. WMO, Geneva, 439 pp.

Wu, J., Y. Kurosaki, M. Shinoda, and K. Kai, 2016: Regional characteristics of recent dust occurrence and its controlling factors in East Asia. *SOLA*, **12**, 187−191.

Yumimoto, K., K. Eguchi, I. Uno, T. Takemura, Z. Liu, A. Shimizu, and N. Sugimoto, 2009: An elevated large-scale dust veil from the Taklimakan Desert: Intercontinental transport and three-dimensional structure as captured by CALIPSO and regional and global models. *Atmos. Chem. Phys.*, **9**, 8545−8558.

Manuscript received 6 December 2018, accepted 24 January 2019
SOLA: https://www.jstage.jst.go.jp/browse/sola/